Large-Scale Airfield Concrete Slab Fatigue Tests

Jeffery R. Roesler[1] Member ISCP, Jacob E. Hiller[2] Member ISCP, and Paul C. Littleton[3]

Abstract

Large-scale concrete slab tests were conducted in the laboratory to evaluate the effect of multiple wheel gears on the fatigue resistance of concrete slabs. Monotonic and cyclic loading was completed on sixteen fully-supported slabs. The monotonic testing characterized the flexural strength of the concrete slab under the fully-supported conditions relative to the standard simply-supported flexural beam test. The testing program addressed the effects of peak stress ratio, stress range, and stress pulse type on the fatigue resistance of concrete slabs. For low cycle fatigue, stress range was not a significant factor while the applied peak stress controlled the number of repetitions to failure. For high cycle fatigue, peak stress and stress range affected the number of cycles to failure. An S-N curve analyses of the fatigue results showed that the number of repetitions to failure for the tridem pulses was not equivalent to the single pulse repetitions to failure for the same pulse duration, peak stress, and stress range.

Introduction

With the onset of new generation aircraft gears, such as the tridem gear, airport pavement design will need to be re-examined to determine the effects of gear spacing and load levels on the development of stresses and resulting fatigue life of concrete slabs. Stress development and fatigue of airport concrete slabs has been researched extensively from Westergaard (1926), the Lockbourne and Sharonville test sections (Parker et al. 1979), the PCA design for airfields (Packard 1973, 1974), and the extensive work by Rollings (1981, 1986, 1990, 1998, 2001) for the U.S. Army Corps of Engineers (USACOE). An extensive review of airfield concrete pavement fatigue can be found in Smith and Roesler (2003) and Littleton (2003).

This fatigue study focuses on comparing large-scale slab results using single and tridem load pulses at various stress ranges with previously published concrete beam and slab fatigue results. Darter (1977), Rollings (1988), Roesler (1998), and Tepfers (1979a, 1979b, 1982) published fatigue equations that will be compared with the results of this study. These fatigue equations will be discussed in more detail in the following section.

[1] Assistant Professor, University of Illinois Urbana-Champaign, Department of Civil and Environmental Engineering, Newmark Civil Engineering Laboratory MC-250, 205 N. Mathews Ave., Urbana, IL, USA 61801 Email: jroesler@uiuc.edu
[2] Graduate Research Assistant, University of Illinois Urbana-Champaign, Department of Civil and Environmental Engineering, Newmark Civil Engineering Laboratory MC-250, 205 N. Mathews Ave., Urbana, IL, USA 61801 Email: jhiller@uiuc.edu
[3] Project Engineer, Applied Research Associates, Inc., 505 West University Avenue, Champaign, Illinois, USA 61820 Email: plittleton@ara.com

Previous Concrete Pavement Fatigue Equations

Concrete Beam Fatigue. In order to develop a design procedure for jointed plain concrete pavements, Darter (1977) compiled 140 fatigue beam results from three published studies Kesler (1953), Raithby and Galloway (1974), and Ballinger (1972) into one least square regression equation:

$$\text{Log}\left(N_f\right) = 17.61 - 17.61\left(\frac{\sigma}{\text{MOR}}\right) \tag{1}$$

where N_f = number of load application until failure, σ = applied maximum stress level, and MOR = modulus of rupture of the concrete.

This beam fatigue equation gives the allowable number of load applications with a 50 percent probability of failure. The Illinois Department of Transportation has employed this fatigue equation into their jointed plain concrete pavement highway design since the early 1990's (Zollinger and Barenberg 1989).

In-service pavements are subject to fluctuating stress range conditions that are brought on by temperature gradients, moisture gradients and varying traffic loads. An important factor to consider in fatigue analysis is the stress ratio (σ_{max}/MOR) and the R-value ($\sigma_{min}/\sigma_{max}$) or stress range in the concrete. Murdock and Kesler (1958) were the first to formally report the effect of R-value on the fatigue life of concrete beams. As the ratio of minimum to maximum stress increased, the concrete could withstand more fatigue cycles at a given stress ratio. At this time, there is no airfield pavement design guide (Portland Cement Association, Tri-service, or Federal Aviation Administration-FAA), which accounts for temperature or directly considers the ratio of the minimum to maximum stress on the fatigue resistance of the concrete.

Several authors (Murdock and Kesler 1958, Aas-Jackobsen 1970, Awad and Hilsdorf 1974, Tepfers and Kutti 1979, Tepfers 1979) have also concluded stress range affects the fatigue resistance of concrete. Aas-Jakobsen (1970) developed a fatigue equation, which accounts for the R-value applied to the specimen:

$$\frac{\sigma_{max}}{f'_c} = 1 - \beta(1 - R)\log_{10} N_f \tag{2}$$

where σ_{max} is the maximum applied stress, f'_c is the compressive or tensile strength of the concrete, and β is a coefficient determined experimentally to be 0.0640.

Domenichini and Marchionna (1981) were one of the first researchers to propose using the applied tensile stress range and stress ratio into concrete pavement design. They modified Tepfers (1979) proposed coefficient (β=0.0685) to account for the variations of in-service pavements that were not accounted for in laboratory-type testing. These differences included varying magnitudes of environmental stresses, rest periods in the field, and variations in concrete field properties such as thickness and strength.

By looking at the effect of R-value on the fatigue life of concrete, it can easily be concluded that it has a large impact on design if considered. Furthermore, the implementation of this into design is difficult, since every fatigue cycle could have a

different peak stress and minimum stress due to the effects of varying temperature and moisture curling and aircraft loading.

Laboratory Concrete Slab Fatigue. Roesler (1998) experimentally investigated the effects of different boundary and support conditions on the fatigue of concrete in the laboratory. Simply-supported beams, fully-supported beams and fully-supported slabs of the same concrete mix were tested to failure at various stress ratios. Simply-supported and fully-supported beam test results had similar fatigue resistance to Darter's (1977) fatigue equation above.

Fully-supported slab fatigue tests were repeatedly loaded at the edge. Test results showed concrete slabs had a higher fatigue resistance than could be predicted by beam fatigue equations. The following regression equation was developed from this research and represents 50 percent probability of fatigue failure:

$$N_f = \left[\frac{1.2968}{(\sigma / MOR_{beam})} \right]^{32.57} \tag{3}$$

In order to explain the difference between slab and beam fatigue results, Roesler (1998) found that the stress ratio (σ_{max} / MOR_{beam}) to cause flexural cracking after one fatigue cycle was around 1.30. This meant that a simply-supported beam strength result could underestimate the flexural strength of a concrete slab by 30 percent for this specific slab thickness. Once the correct flexural strength of the concrete slab was used in the stress ratio calculation then all three specimen geometries and configurations produced similar fatigue curves.

Field Concrete Slab Fatigue. To further improve the design procedures for the FAA and USACOE especially for overlays, Rollings and Witczak (1990) published an updated concrete fatigue equation based on the structural condition index (SCI) and layered elastic analysis of rigid airfield pavements. The primary thrust of the research was combining the USACOE layered elastic design for new rigid pavements with rigid overlays on existing rigid pavements. The SCI includes only distresses resulting from structural failure. The following are the two equations published by Rollings (1988) to describe fatigue failure using the SCI concept:

$$DF = 0.5234 + 0.3920 * \log(C100) \tag{4}$$

$$DF = 0.2967 + 0.3881 * \log(C0) \tag{5}$$

C100 is defined as the coverages for the SCI to drop below 100 and C0 is the coverages required to reduce the SCI of the pavement to zero. DF is the design factor defined as MOR/σ, which is also the inverse of stress ratio. Interpolation can be completed for allowable coverage at intermediate SCI values. Equation (4) is referred as "first crack", while equation (5) is referred to as "shattered slab" in this paper. The FAA adopted these fatigue equations for use in their LEDFAA program (FAA 1995).

Experimental Test Plan

In order to explore the effect of stress range and stress ratios on the fatigue resistance of airfield concrete pavements, a test plan was developed to repetitively load large-scale concrete slabs on top of a 20cm natural clay subgrade contained in a laboratory test frame. A total of sixteen slabs, measuring 2.0m by 2.0m by 15cm thick, were cast for the testing program. Strain gages were embedded in the slabs to measure load-induced strains and linear variable differential transducers (LVDTs) were positioned on top of the slabs to record deflections during testing.

The test plan included both single and tridem mid-slab edge haversine load pulses (see Figure 1) along with three stress ranges (R=0.1, 0.4, and 0.7) and two stress ratios (1.0 and 1.3, based on beam strengths). The single load pulse was designed to be at a frequency of 2Hz with no unloading between pulses, as seen in Figure 1. Three peak stresses comprised the tridem load pulse with the R-value signifying the ratio between the minimum stress and maximum stress as shown in Figure 1. The tridem pulse duration was one second with 3 peak stresses (3 Hz). The unloaded stress for the tridem pulse was always 10 percent of the maximum load. The tridem pulse frequency corresponded to a velocity of 31.2 kph for a typical Boeing 777 aircraft at an axle spacing of 1.45 m. The comparison between single and tridem slab tests in fatigue will be used to determine how to account for tridem load pulses in a fatigue counting scheme for rigid airfield pavements.

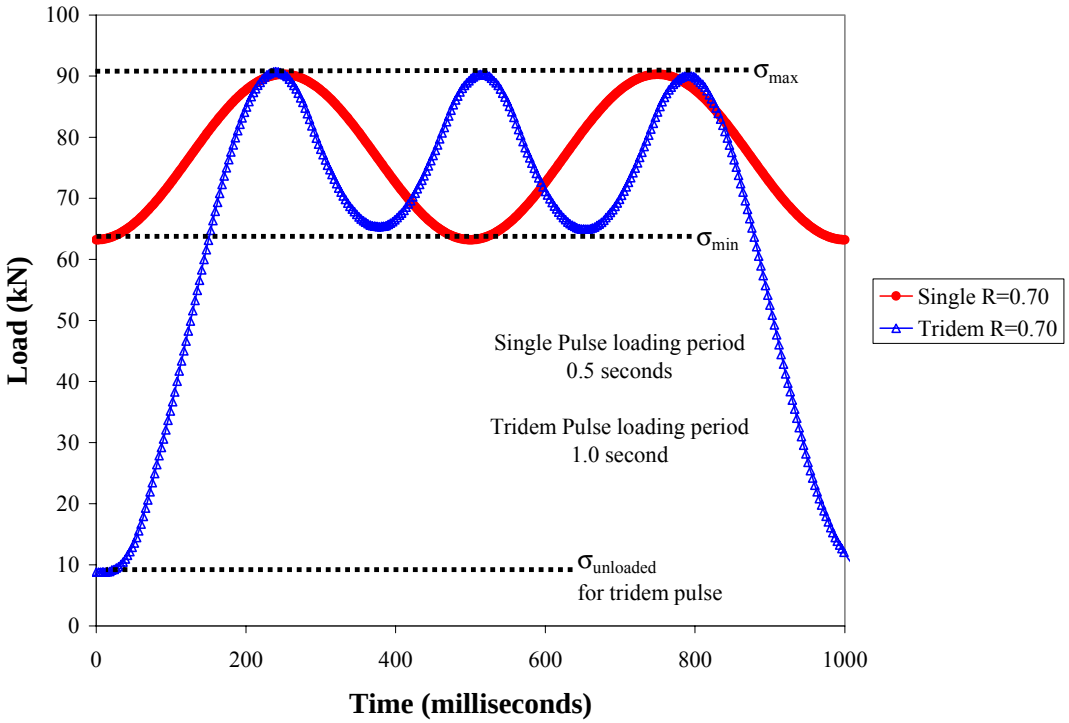


Figure 1. Example of Single and Tridem Load Pulses (R=0.70).

Test Setup. Testing of the concrete slabs was conducted utilizing a custom design testing frame and soil containment box located at the University of Illinois' ATREL facility in Rantoul, Illinois (Figure 2). A hydraulic actuator transmitted the load to

the slab through a 20.3cm by 20.3cm by 2.5cm thick steel platen. The subgrade was a layer of low-plasticity clay, which was contained inside a 5.1m long by 2.4m wide by 30.5cm deep steel box supported by the base of the frame. The soil had a CBR value of 5 at 17 percent moisture content. To prevent moisture loss, the clay was covered with 6-mil polyethylene sheeting. The first two slabs (slab numbers 1 and 2) were cast directly on top of the sheeting whereas the remaining slabs were cast in wood forms, cured, and then placed in the frame on top of the sheeting, under which approximately 1 to 2cm of sand was used to maintain full contact between the slab and subgrade.



Figure 2. Test frame and soil containment box.

The vertical slab deformations, bending strains in the slab, and the applied force were measured and collected electronically. The locations of the LVDTs and strain gages are shown in Figure 3. A custom designed computerized control program was used to activate testing and acquire measurement data in real time.

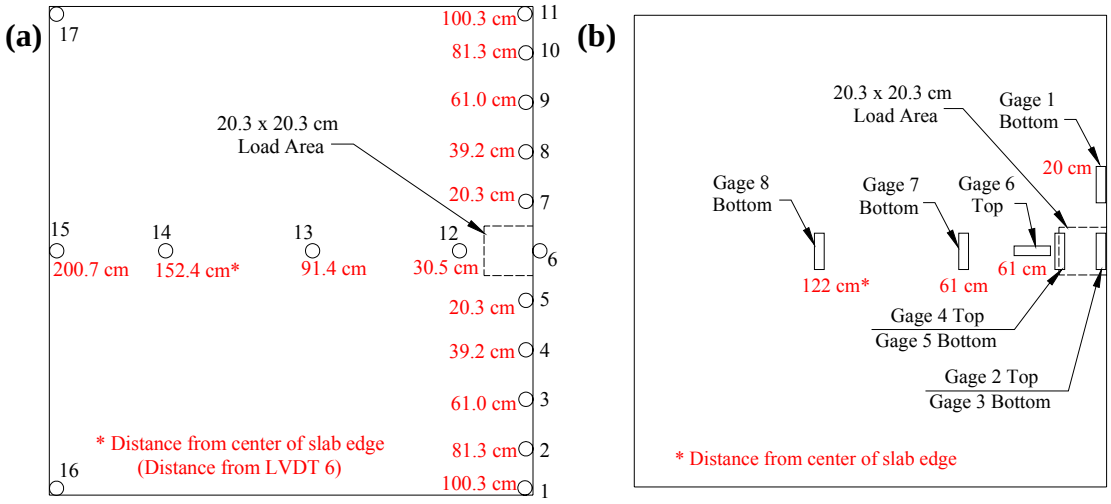


Figure 3. Slab Instrumentation Layout for (a) LVDTs and (b) Strain Gages.

Materials. Typical airfield concrete was obtained from a local ready mix supplier and was similar to previous designs used by several regional airports in Illinois (see Table 1). Coarse aggregate used in the mix was a crushed limestone with a 2cm nominal size and the fine aggregate was natural sand. Water to cement ratio was 0.40 and the entrained air content was approximately 4.0 percent. Specimens for flexural and compressive strength testing were also cast and tested periodically at similar ages as the corresponding slab tests.

Table 1. Concrete Mix Design and 28-Day Strengths

	Slabs 1 & 2	Slabs 3 - 9	Slabs T1-T7
Date Cast	4/23/2002	8/8/2002	10/10/2002
Coarse Aggregate (kg/m^3)	1092	1085	1085
Fine Aggregate (kg/m^3)	651	707	707
Type I Cement (kg/m^3)	291	290	290
Type C Fly Ash (kg/m^3)	92	77	77
Water (kg/m^3)	154	145	145
w/c	0.4	0.4	0.4
Entrained Air (%)	4.0 (estimated)	4.0 (measured)	4.0 (measured)
f'_c (MPa)	44.1	23.7	36.4*
MOR_{beam} (MPa)	4.2	3.0	4.7*

* Measured at 90 days

Definition of Cracking and Slab Failure. Published research has many ways of defining slab failure. The cycles until initial cracking in beams has been used synonymously with the concrete's fatigue life. However, for an indeterminate structure, like a concrete slab-on-grade, cycles at which first cracking occurs is not necessarily the same as the fatigue life.

For this research, initial slab cracking was defined by the first appearance of a hairline crack and/or a change in strain behavior. The fatigue cycle in which the initial crack occurred was recorded, but typically the testing was continued to try and achieve the flexural failure of the edge-loaded slab. Slab flexural failure was defined as the point where the concrete slab fully-hinged along one axis of the slab. The main difference between slab and beam testing is the additional cycles required to drive an initial crack through the slab depth and across the bottom of the slab whereas a simply supported beam will fail without the occurrence of a visual crack.

Slab Testing in Fatigue and Monotonic Loading

Table 2 shows testing parameters and results from the single haversine load pulse testing (Slabs 1-9) at 2 Hz. Due to prolonged fatigue resistance, slabs 1, 5 and 6 received multiple loading schemes. Slab 1 underwent a fatigue test (1a), which did not result in cracking so a monotonic test (1b) was conducted to obtain the flexural strength of the slab (MOR_{slab}). Slabs 5 and 6 did not crack in the first fatigue test (5a and 6a), therefore a second fatigue test was conducted on each slab, which was recorded as tests 5b and 6b. The second fatigue test on these two slabs only produced initial cracking. Failure was accomplished through monotonic tests 5c and 6c for which the maximum load at failure was obtained.

Table 3 shows the monotonic and fatigue data for the tridem load pulse testing. The slabs were numbered T1 through T7 with only slab T5 receiving multiple load schemes. Slab T5 did not fail under increasing stress ratios and therefore a monotonic test (T5m) was conducted to obtain the strength of the slab.

To determine the bending stress in the slab, each slab's rebound deflection profile was matched with the finite element program ISLAB2000 (Khazanovich et al. 2000) at 10 percent of the slab's fatigue life. Slabs 7 through 9, T3, T6, and T7 began crack initiation and propagation from the commencement of cyclic loading and thus the deflection profile during the initial fatigue cycles was utilized in the stress calculation. The maximum and minimum bending stresses from ISLAB2000 were recorded once the input deflection values were matched to actual test deflection values. Deflection values were matched by changing only the modulus of subgrade reaction (k-value).

The varying of k-value between slabs in both the single and tridem load pulse testing program, as seen in Tables 2 and 3, is reasonable since each slab was separately loaded into the soil containment box and thus the exact support condition beneath the slab was not the same for each slab test. Furthermore, backcalculated k-values determined from the static and dynamic testing of the concrete slabs where significantly different ranging from 17.4 kPa/mm to 90.1 kPa/mm for static monotonic testing and 27.1 kPa/mm to 468 kPa/mm during dynamic fatigue testing.

Table 2. Summary of Single Pulse Test Results.

	1a	1b	2	3	4	5a	5b	5c	6a	6b	6c	7	8	9
Test Type	Fatigue	Mono	Mono	Mono	Fatigue	Fatigue	Fatigue	Mono	Fatigue	Fatigue	Mono	Fatigue	Fatigue	Fatigue
Test Date*	11-Jun	15-Jun	16-Jun	12-Sep	15-Sep	27-Sep	4-Oct	10-Oct	26-Oct	29-Oct	31-Oct	12-Nov	26-Nov	7-Dec
MOR_{beam} (MPa)	4.2	4.2	4.2	3.6	3.8	4.3	4.5	4.6	4.7	4.7	4.7	4.7	4.7	4.7
MOR_{slab} (MPa)	12.2	12.2	10.7	9.5	9.5	13.2	13.2	13.2	13.2	13.2	13.2	13.2	13.2	13.2
k-Value (kPa/mm)	299	41	19	18	107	299	250	90	468	409	17	98	27	319
σ_{max} / MOR_{beam}	0.83	--	--	--	1.8	1.38	1.62	--	1.63	1.83	--	2.27	2.5	1.76
σ_{min} / σ_{max}	0.1	--	--	--	0.1	0.4	0.4	--	0.7	0.7	--	0.1	0.4	0.7
σ_{max} / MOR_{slab}	0.3	--	--	--	0.7	0.5	0.6	--	0.6	0.7	--	0.8	0.9	0.6
Fatigue Crack Initiation	--	--	--	--	5,000	--	55,296	--	512	NA	--	1	1	1
Cycles Tested to	--	--	--	--	143,896	999,936	611,328	--	465,920	144,640	--	64	7	352
Cycles at Failure (N_f)	--	--	--	--	143,896	--	--	--	--	--	--	64	7	352
P_{max} (kN)	44.9	210	160.1	86.3	69.4	68.5	81.8	--	95.6	105	--	107.2	109	96.5
P_{min} (kN)	4.4	--	--	--	6.2	27.1	32	--	66.7	73	--	9.8	43.6	67.6
P-Ratio (P_{max} / P_{slab})	0.2	--	--	--	0.8	0.5	0.6	--	0.8	0.9	--	0.9	0.9	0.8

*All tests in Table 2 performed in year 2002.

Table 3. Summary of Tridem Pulse Test Results.

	T1	T2	T3	T4	T5a	T5b	T5c	T5d	T5m	T6	T7
Test Type	Mono	Fatigue	Fatigue	Fatigue	Fatigue	Fatigue	Fatigue	Fatigue	Mono	Fatigue	Fatigue
Test Date*	10-Jan	6-Feb	4-Mar	18-Mar	15-Apr	8-May	15-May	19-May	20-May	22-May	28-May
MOR_{beam} (MPa)	4.7	5.2	4.9	5	5.6	5.6	5.6	5.6	5.6	5.6	5.6
MOR_{slab} (MPa)	13	13	13	13	14.4	14.4	14.4	14.4	15.7	14.4	14.4
k-value (kPa/mm)	27	109	109	109	109	109	109	109	27	109	109
σ_{max} (MPa)	13	8.5	8.3	8.4	8	8.6	9.2	9.8	15.7	9.1	8.3
σ_{min} (MPa)	--	0.7	4.1	6.1	0.7	0.8	0.8	0.9	--	4.2	6
$\sigma_{unloaded}$ (MPa)	--	0.7	0.8	0.7	0.7	0.8	0.8	0.9	--	0.9	0.7
σ_{min} / σ_{max} *(theoretical)*	--	0.1	0.4	0.7	0.1	0.1	0.1	0.1	--	0.4	0.7
σ_{min} / σ_{max} *(actual)*	--	0.08	0.49	0.72	0.08	0.09	0.09	0.09		0.47	0.72
σ_{max} / MOR_{beam}	2.8	1.63	1.69	1.68	1.41	1.52	1.63	1.73	2.79	1.61	1.48
σ_{max} / MOR_{slab}	--	0.65	0.64	0.65	0.55	0.6	0.64	0.68	--	0.63	0.58
Fatigue Crack Initiation	--	47,136	1	992	--	--	--	--	--	1	1
Cycles Tested to	--	61,184	1	4,384	500,064	521,280	500,064	262,656	--	26,240	5,440
Cycles at Failure (N_f)	--	61,184	1	4,384	--	--	--	--	--	26,240	5,440
P_{max} (kN)	128.6	91.2	89.4	90.3	78.7	84.5	90.7	96.5	155.2	89.9	89.4
P_{min} (kN)	--	7.6	44	64.9	6.7	7.6	8	8.5	--	41.8	64.5
$P_{unloaded}$ (kN)	--	7.6	8.9	8	6.7	7.6	8	8.5	--	8.5	7.6
P_{slab} (kN)	128.6	128.6	128.6	128.6	141.9	141.9	141.9	141.9	155.2	141.9	141.9
P-Ratio (P_{max} / P_{slab}) (theoretical)	--	0.75	0.75	0.75	0.65	0.7	0.75	0.8	--	0.65	0.65
P-Ratio (P_{max} / P_{slab}) (actual)	--	0.71	0.69	0.7	0.55	0.6	0.64	0.68	--	0.63	0.63

*All tests in Table 3 performed in year 2003.

Slab Testing Discussion

Beam versus Slab Flexural Strength. As seen in Tables 2 and 3, slab strengths were considerably higher than beam strengths tested at the same age of curing. Roesler (1998) found that fully supported slabs (15cm thickness) under edge loading were 30 percent stronger than companion beams tested in 3rd point bending. The concrete slabs' flexural strength were on average 2.8 times the strength of simply-supported beams. This confirms that the slab to beam strength ratio depends on the concrete specimen thickness, slab geometry, loading configuration, and boundary conditions.

Single Pulse Testing Comparison to Existing Fatigue Curves. S-N curves have been used to relate the number of cycles to fail a specimen (N_f) to the ratio between applied stress and the concrete flexural strengths (S). An S-N curve using the concrete beam strength is plotted in Figure 4 for the single pulse fatigue results.

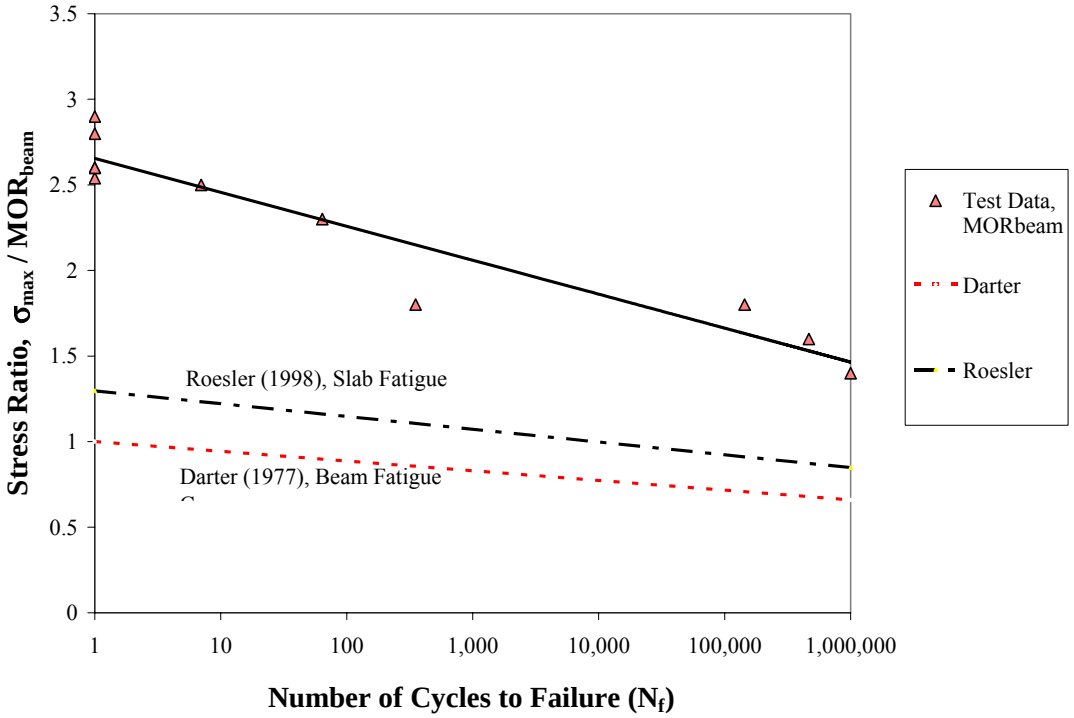


Figure 4. Comparison of Single Pulse Slab Test Data with Previous Laboratory Fatigue Curves.

The concrete beam fatigue curve of Darter (1977) is also plotted to illustrate how the fully supported concrete slabs produces a higher fatigue resistance relative to simply-supported beam fatigue results. The slab fatigue curve in Figure 4 developed by Roesler (1998) also found slabs to have greater fatigue resistance than predicted by concrete beam tests. Figure 4 shows laboratory slab fatigue tests of the same thickness do not produce comparable fatigue curves if the boundary conditions and stress range are different. The current tests were finite-sized slabs (2m by 2m) with no edge restraints and three stress ranges (0.1, 0.4, 0.7). The slabs tested by Roesler (1998) were 1.2m square and configured to behave like infinite slabs through

application of edge restraints. All the slabs tested by Roesler (1998) had R-values of 0.10. The differences in boundary conditions and larger stress range are the main reasons the results by Roesler (1998) failed faster than the current slab tests in this study.

For slab fatigue testing, Roesler (1998) found by using the flexural strength of the slab configuration in the stress ratio instead of the beam flexural strength, the slab fatigue data resembled the beam fatigue curve of Darter (1977) as shown in Figure 5. By normalizing the new fatigue data relative to the concrete flexural strength of the test configuration being used in this study, the fatigue data showed similar behavior to the Darter (1977) beam fatigue curve and previous slab tests by Roesler (1998).

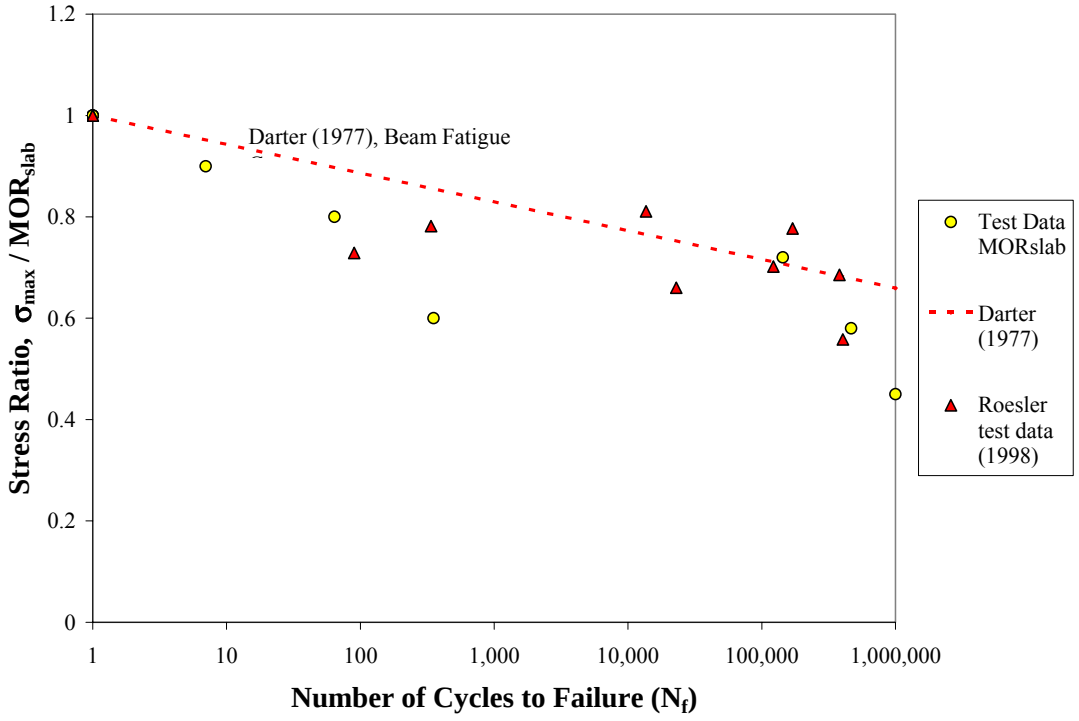


Figure 5. Comparison of Fully Supported Slab Fatigue Test Data and Beam Fatigue Curve Based on Slab MOR.

Tridem Pulse Testing Comparison to Existing Fatigue Curves. In Figure 6, the resulting S-N curve for the tridem testing is shown. Tridem load applications and the tridem load applications multiplied by three are shown in an attempt to determine how to account for these load pulse types in comparison with single pulse loads from previously published fatigue transfer functions. Like the single pulse testing, the resulting tridem test data does not appear to match previously published fatigue relationships, which appear extremely conservative from this data.

In Table 3, the stress ratios for tests that produced fatigue failure ranged from 1.48 to 1.69. This small range of stress ratios provided little clarity in trying to determine the overall effect of stress ratio to the number of cycles until failure. The resulting trendlines for both the tridem cycles and the tridem cycles counted as three

load applications appear almost flat if the monotonic tests (N_f =1 data) were not accounted for in the S-N plot. In comparison, the Darter, Roesler, and Rollings fatigue functions predict a clear increase in repetitions with a lower stress ratio. The tests for Slab T5 (T5a, T5b, T5c, and T5d) produced no failure in fatigue and are noted by the hollow data points. The stress ratios for these tests ranged from 1.41 to 1.73 and were increased as the test on Slab T5 was conducted in an attempt to fail the slab. If these tests at the lower stress ratio were run to failure, then possibly a clearer trend in the S-N curve for this test data could be noted as was seen in the single pulse data shown in Figure 4.

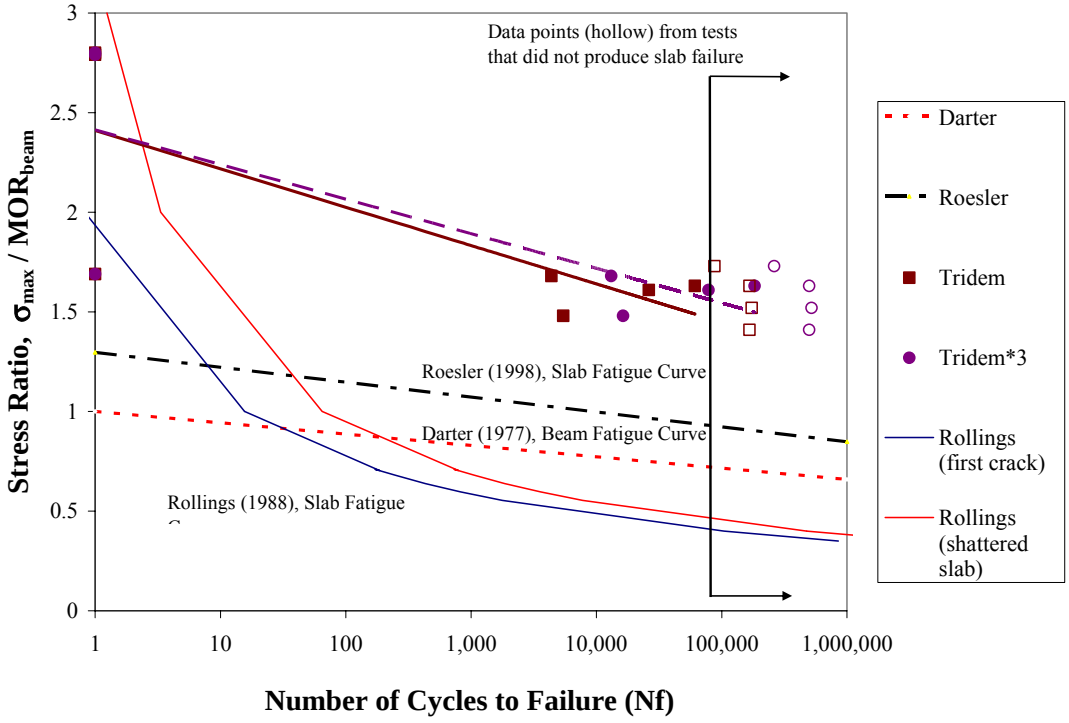


Figure 6. Comparison of Tridem Slab Test Data with Previous Fatigue Curves.

Particularly at the later stages of several tests, an observed uplift of the side of the slab opposite the edge load was noticed in addition to microcracking (indicated by strain gage reading changes) near the load. These conditions resulted in the slab significantly punching into the subgrade, thereby altering the estimated k-value as more fatigue cycles were applied. Numerous centerline profiles (see Figure 7a) from surface LVDT readings verify that after some loading the slab was undergoing a punching into the subgrade for the first 0.5 to 0.9m of the slab nearest the loaded edge, which clearly brought another variable into play. The inconsistency of the amount of rotation due to the loaded edge induced different stress states that could not be directly accounted for. The change in support conditions between slabs was found to be a major factor in determining the number of cycles to failure.

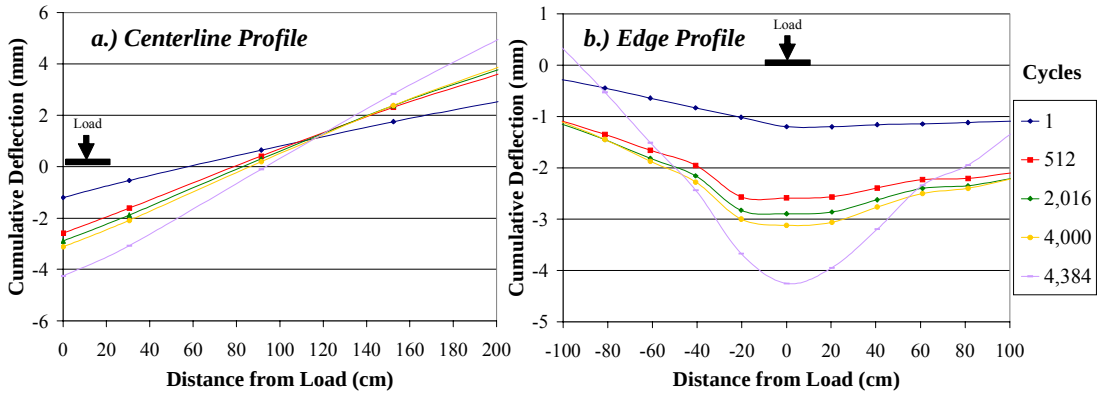


Figure 7. Centerline (a) and Edge (b) Profiles for Slab T4 Under Fatigue Loading.

Due to significant slab punching into the subgrade, a P-ratio (P_{max}/P_{slab}) was explored to relate the fatigue testing load level to the load required to produce the maximum monotonic strength of the slab in order to circumvent the potential stress miscalculations and resulting stress ratios. However, the P-ratio did not address the microcracking detected near the loaded area, localized increase in subgrade support conditions, or inherent material variability from slab to slab. Figure 8 shows the resulting tridem load pulse results in terms of P-ratio in comparison to Rollings (1988), Darter (1977), and Roesler's (1998) functions for concrete pavement fatigue.

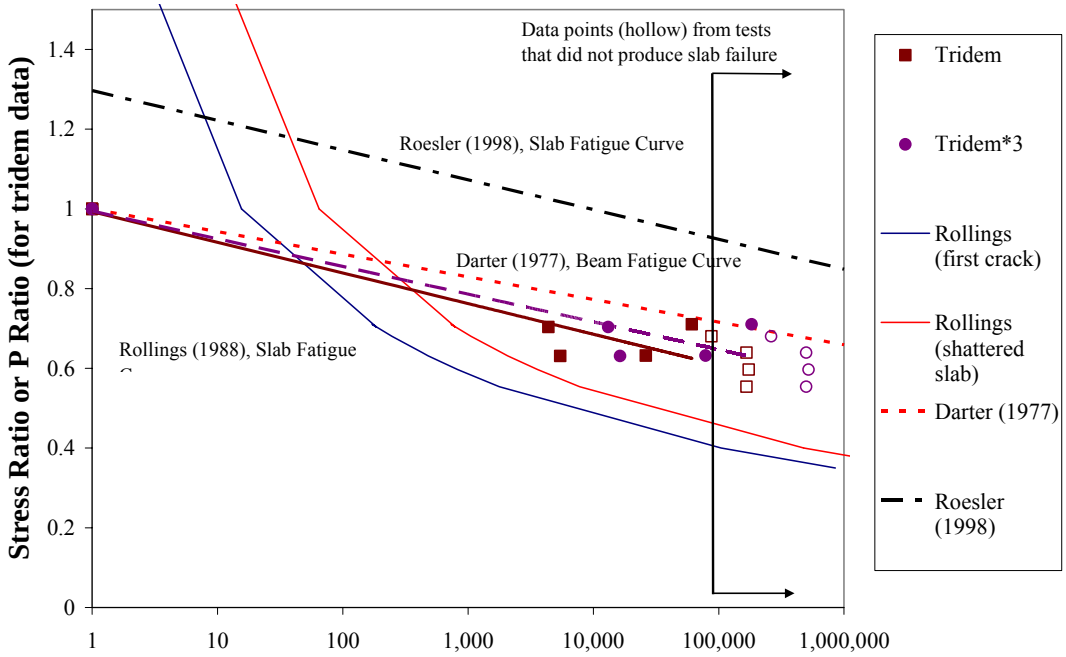


Figure 8. Comparison of Tridem Slab Test Data using P-Ratio with Rollings' Fatigue Functions.

One inherent difference in using the P-ratio to compare against slab fatigue functions can be found during extremely low cycle fatigue. The P-ratio is limited to a maximum of 1.0, as the slab should immediately crack when it is loaded to its flexural load carrying capacity. In contrast, Rollings' functions are developed from the stress in the pavement slab with respect to the strength of a concrete beam. Due to the geometric size-effect and boundary condition differences, the strength of the beam is far less than the slab strength and the resulting stress ratios can be far above 1.0. Even when comparing the high cycle fatigue data from the tridem testing to Rollings' fatigue functions, the existing fatigue transfer functions appear to be quite conservative at higher allowable repetitions. The stresses calculated for the Rollings' fatigue functions are calculated from layered elastic analysis unlike the method for stress calculation used in this analysis. The built-in reliability level of the Rollings' functions is unknown and may lead to the conservative fatigue life prediction at repetition to failure greater than 100. By setting the assumption of a P-ratio of 1.0 equals failure after one application, the resulting plots from Figure 8 mirror the Darter equation quite well considering the R-value was ignored and the small number of data points.

Effects of Stress Range in Single and Tridem Pulse Testing. One of the main variables used in both the single and tridem pulse testing schemes was the range of stress experienced between peaks loadings. This was accounted for by the R-value and was intended to be at the levels of 0.10, 0.40, and 0.70.

One method for determining the effect of stress range on concrete slabs is viewing the strain responses during loading. One interesting phenomenon from the strain readings throughout the tests was the reduction in strain response between peaks as the fatigue cycles accumulated. Figure 9 shows the strain readings for the 1st, 448th (10% N_f), and 4,352nd tridem cycle (failure) for Slab T4 (R=0.70). During the first tridem cycle, it can be seen that when 70 percent of the load is still applied between the three peak loads, the strain levels of Gages 3 (mid-slab edge under the load platen) remains at roughly 65 percent of the maximum strain level. However, as the load applications continue and the crack begins to propagate in the slab, the strain levels relax to levels approaching zero, even though the load level remains at 70 percent of the maximum load between peak loads. At 448 cycles and at flexural failure, this minimum strain level is roughly 20 percent of the maximum strain level.

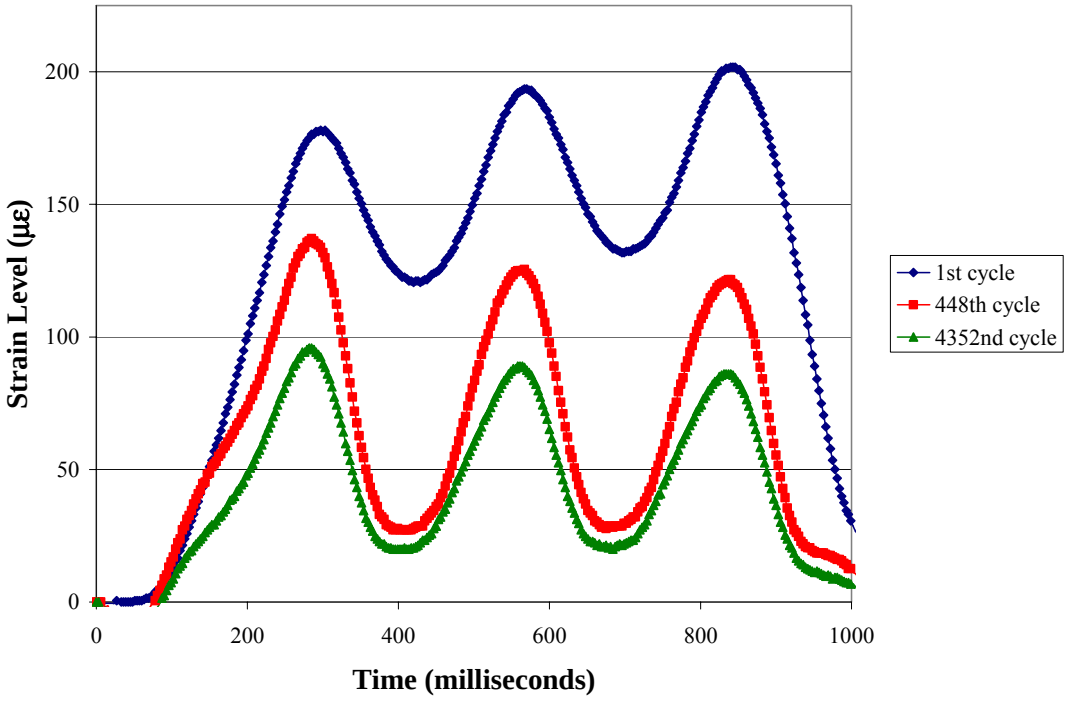


Figure 9. Strain Gage #3 Readings for Slab T4 (R=0.70) Under Fatigue Loading.

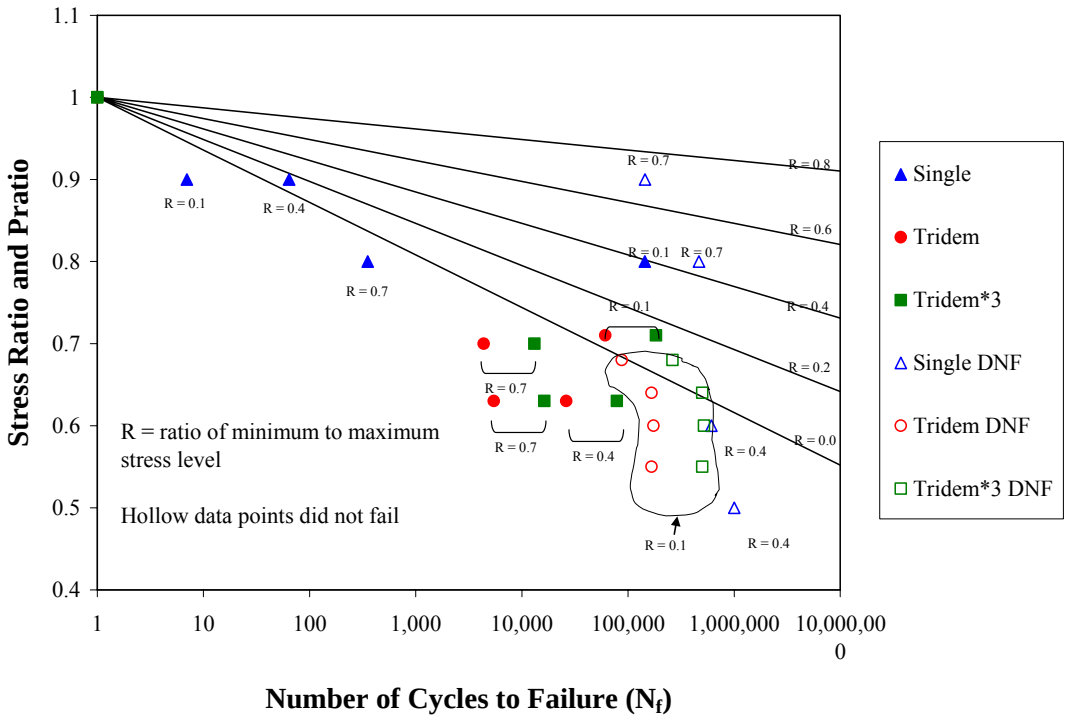
Crack initiation was visually noticed on Slab T4 after the 992nd tridem load pulse. However, this crack was extremely small and strain readings for critical gages remained engaged for some time after this initial cracking. This suggests that the driving force for the crack to propagate near the crack tip had relaxed somewhat by the 448th cycle allowing both the maximum and in-between peak strain levels to diminish. This would imply that early in the fatigue process, the tridem load pulses do not fully behave as three separate load pulses as the strain levels remain high even between peak tridem load pulses. However, this reduction in the in-between peak strain levels later in the fatigue process allows the slab responses to more fully cycle as three distinct pulses and should be counted as such in a fatigue relationship. This would agree with Rao and Barenberg (2000) who suggested that pavements experience more load cycles than anticipated when tridem load pulses are applied in comparison with single pulse loads. Studies of both the FAA National Airport Pavement Test Facility (Rao and Barenberg 2000) and the Denver International Airport (Fang 2000) indicated that, under tridem gears loadings, the concrete slabs were subjected to compression cycles as the load was approaching (full compression-tension strain reversals) and low R-values between peak loads of the tridem gear.

One major factor in assessing the impact of stress range using the R-value is the resulting subgrade compression. At higher R-values, the minimum load level applied to the slabs remains high, thereby not allowing for the subgrade to recover elastically as seen earlier in Figure 7b. This effectively changes the boundary conditions of the test during the higher R-value test as well as between tests at different R-values as the underlying layers do not have time to recover under cyclic

load conditions. This effect is further amplified after initiation of the crack as the stress on the subgrade is dramatically increased. From Figures 7a and 7b, it can be seen that the subgrade undergoes significant compression under the loaded area. These changing subgrade boundary conditions make the effect of the load-induced R-value on slab fatigue less clear.

Under field conditions, the minimum residual stress from temperature curling and built-in curl effects does not produce these significant permanent deformations in the underlying layers. Therefore, extrapolating the results of high, load-induced R-values may not be representative of the true impact of stress range on in-service concrete slab fatigue with respect to temperature and moisture curling.

Comparison of Single Pulse and Tridem Results. Figure 10 shows the tridem pulse loads counted as both one load repetition (red circle) and three repetitions (green square), while the single load pulse data points are designated as blue triangles. From a stress range perspective, the damage from a tridem pulse should be more than a single pulse, but less than three single pulses as the load level does not dissipate down to the minimum level under all R-value tests. The tridem tests were performed at lower P-ratios, which would suggest a higher cycle fatigue scenario than most of the single load pulse tests. As seen in Figure 10, the tridem tests do not match up with the Tepfers and Kutti (1979) stress range relationship using the P-ratio concept very well. Looking at tests around a stress range of 0.63 to 0.67, the test with the highest R-value of 0.70 failed the earliest, while the corresponding test at R=0.10 did not fail and required an increase in the stress ratio (or P-ratio) for further testing. This abnormality may be due to the reduction of the load level to a minimum of 10 percent of the maximum load after each load pulse and the greater permanent deformation occurring at the higher minimum sustained stress level. Due to the nature of semi-logarithmic plots such as Figure 10, the small differences in the R=0.10 and R 0.40 test results at P-ratio near 0.63 are also exacerbated graphically.



Number of Cycles to Failure (N_f)

Figure 10. Single and Tridem Pulse Fatigue Results Plotted on Tepfer's S-N Fatigue Relationship for Concrete Stress Range.

From visual analysis of Figure 10, it can also be noticed that the applied P-ratio (or stress ratio) appears to be the more dominant component in comparison to stress range in determining the number of cycles to failures for both the single and tridem load pulses. Disregarding the stress range effects, the plotted results demonstrate a general trend of increased fatigue life with lower maximum applied stress, as expected. Under a more controlled test, such as in simply-supported beam, issues such as stress range and load pulse type can more easily be distinguished since the support condition does not change throughout crack initiation and propagation. The changing subgrade support potentially overshadows the resolution required to see the stress range and load pulse type effects in the slab fatigue testing.

Figure 11 shows single and tridem test results plotted against the Darter, Roesler, and Rollings' concrete fatigue relationships using beam strength in the stress ratio calculations. The fatigue results from the single and tridem pulse loading did not correlate well with any of the existing fatigue equations except the general trend of increased life with decreased stress ratio. These large discrepancies are most attributed to difference in the stress calculation, geometric and boundary condition differences, and failure definitions. Disregarding Slab T3 under the tridem testing program that failed unexpectedly after one repetition, the trendline depicting single pulse load results tend to match the tridem test results better when these loads are counted as three distinct pulses instead of just one pulse. These trendlines did not consider slabs that did not fail in fatigue.

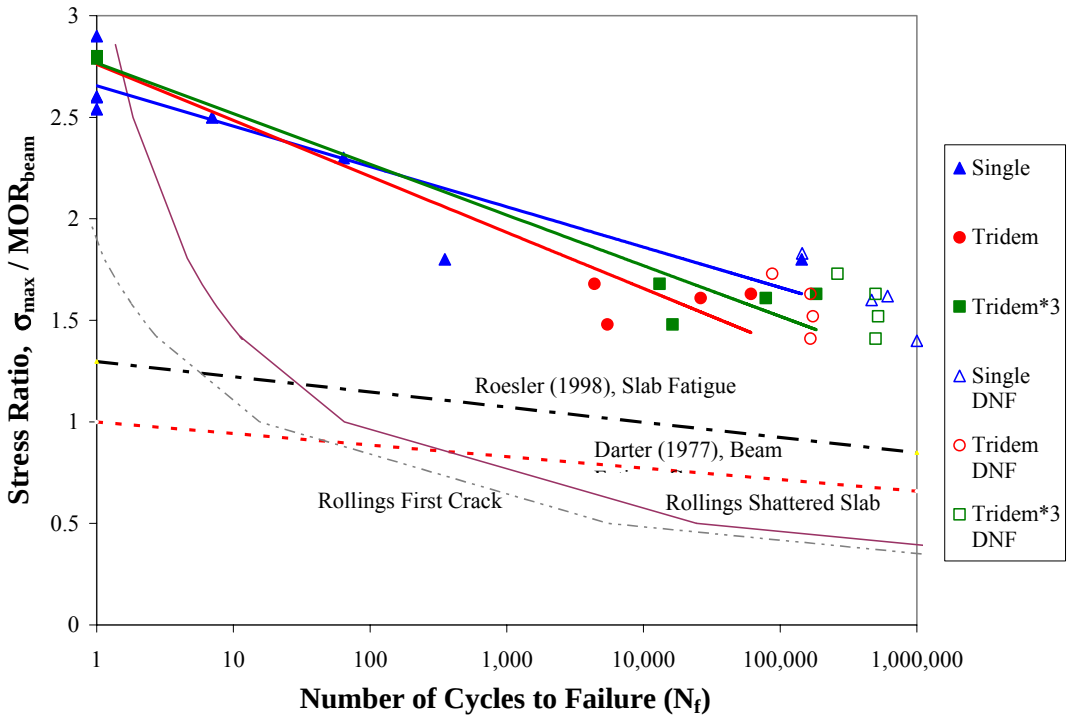


Figure 11. Single and Tridem Pulse Fatigue Results Plotted on Darter, Roesler, and Rollings' Fatigue S-N Relationships using Beam Strength.

When using the slab's flexural strength instead of the beam flexural strength in the applied stress ratio calculations (Figure 12), the data tend to match the existing beam fatigue relationship much better. In Figure 11, the single pulse and the tridem trendlines match almost exactly when the tridem cycles are counted as three distinct load pulses. This would substantiate the theory that the strain levels in-between the three peaks of the tridem pulses tended to minimize during low-cycle fatigue testing near the crack initiation areas, thereby producing three nearly-complete load-unload strain pulses as load cycles were increased. When plotted in this format, the results of the slabs tested to failure follow the Darter (1977) fatigue curve fairly well, while the slopes of the trendlines match the slope of Roesler's slab fatigue prediction within 5 percent. The laboratory data does not match either of Rollings' field slab fatigue life predictions.

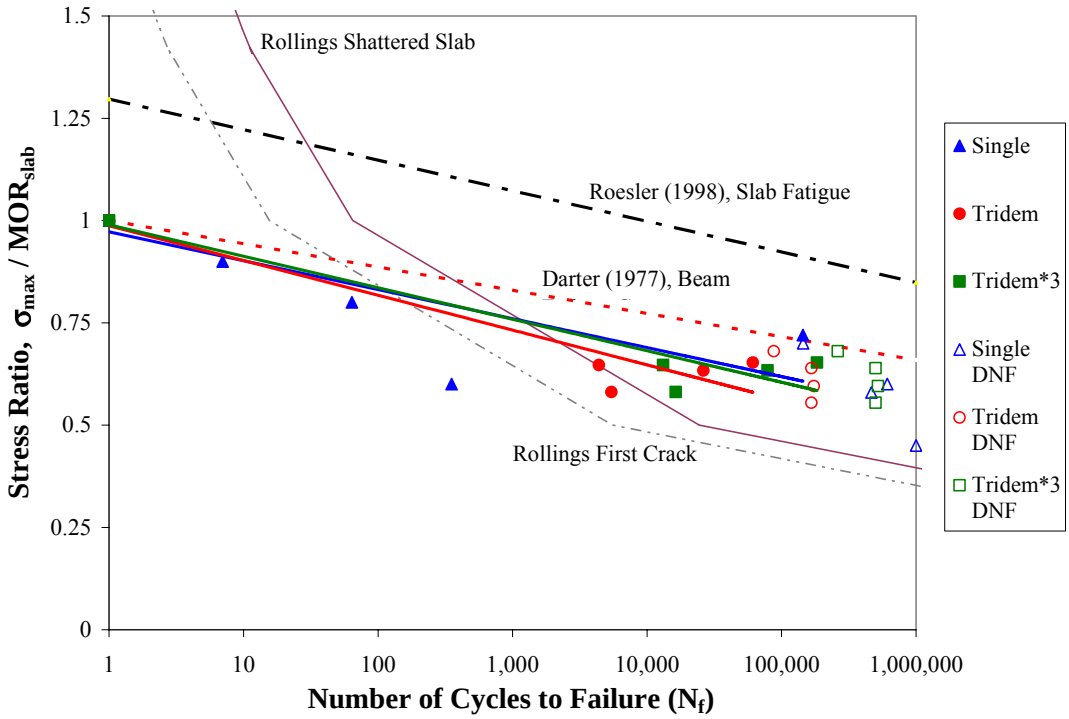


Figure 12. Single and Tridem Pulse Fatigue Results Plotted on Darter, Roesler, and Rollings' Fatigue S-N Relationships using Slab Strength.

Conclusions

Many studies have characterized the fatigue behavior of airfield concrete pavements through full-scale field testing, laboratory slab testing, or beam testing. From this fatigue data, researchers have developed concrete fatigue transfer functions (S-N curves) to assist in the thickness design of airfield concrete pavements. The FAA has designed pavement thicknesses based on low cycle fatigue (<10,000 coverages) curves derived from field tests conducted by the USACOE. For this study, a testing program was conducted to determine the fatigue resistance of concrete slabs subjected to various stress ratios and ranges for both a single and tridem load pulse.

The concrete slab fatigue tests confirmed beam fatigue curves could not be used to accurately predict fatigue failure in concrete slabs. S-N fatigue curves for concrete slabs are shifted higher than beam fatigue curves. The main reason for beam and slab fatigue curve discrepancy was the estimation of the flexural strength of the concrete slab. For testing under these boundary conditions and geometry, slab flexural strength was found to be approximately 2.8 times greater than the companion beam flexural strength.

Concrete slab fatigue curves were found not to be unique and depended on the specific boundary conditions and slab geometry tested. A single slab fatigue curve cannot be used to accurately predict the fatigue life of concrete pavements using the traditional stress ratio (applied stress/beam strength) approach. Stress range did not significantly influence the concrete slab's fatigue life during this testing program.

With high stress ratios, the subgrade support condition changed progressively, which overshadowed the effect of stress range on concrete slab fatigue resistance.

When the slab fatigue tests were plotted in terms of applied load to maximum failure load (P-ratio) in an attempt to eliminate differences in boundary conditions between tests, the slab fatigue curve resembled the classic beam fatigue curve published by Darter (1977). The use of stress ratio with the slab strength also proved to be more depictive of classic fatigue relationships than using beam strength values. In order to accurately predict the fatigue life of a concrete slab, the concrete slab flexural strength (for a given geometry and boundary conditions) must be known.

Acknowledgements

This paper was prepared from a study conducted in the Center of Excellence for Airport Technology. Funding for the Center of Excellence is provided in part by the Federal Aviation Administration and is located at the University of Illinois at Urbana-Champaign, with partners at Northwestern University and the Federal Aviation Administration. The financial and technical assistance received for this project is greatly appreciated.

References

Aas-Jakobsen, L. (1970), "Fatigue of Concrete Beams and Columns," *Bulletin No. 70-1*, Division of Concrete Structures, NTH, Trondheim.

Awad, M.E. and Hilsdorf, H.K (1974), "Strength and Deformation Characteristics of Plain Concrete Subjected to High Repeated and Sustained Loads," *Abeles Symposium, Fatigue of Concrete*, ACI Publication SP-41, pp. 1-13.

Ballinger, C.A. (1972), "Cumulative Fatigue Damage Characteristics," *Highway Research Record No. 370*, Highway Research Board, National Research Council, pp. 48-60.

Darter, M.I. (1977), *Design of Zero-Maintenance Plain Jointed Concrete Pavement, Volume 1: Development of Design Procedures*, Federal Highway Administration Report No. FHWA-RD-77-III.

Domenichini, L. and Marchionna, A. (1981), "Influence of Stress Range on Plane Concrete Pavement Fatigue Design," *Proceedings of the Second International Conference on Concrete Pavement Design*, Purdue University, West Lafayette, IN, pp. 55-65.

Fang, Y. (2000). "Analysis of Load Responses in PCC Airport Pavement." *International Journal of Pavement Engineering,* Vol. 1, No. 1, pp. 1-14.

Federal Aviation Administration (1995), *Airport Pavement Design for the Boeing 777 Airplane,* Advisory Circular 150/5320-16.

Foxworthy, P.T. (1985), *Concepts for the Development of a Nondestructive Testing and Evaluation System for Rigid Airfield Pavements*, Ph.D. Thesis, University of Illinois, Urbana, Illinois.

Kesler, C.E. (1953), "Effect of Speed of Testing on Flexural Fatigue Strength of Plain Concrete," *Proceedings, Highway Research Board*, Vol. 32, pp. 251-258.

Khazanovich, L., Yu, H.T., Rao, S., Galasova, K., Shats, E., and Jones, R. (2000). *ISLAB2000 – Finite Element Program for Rigid and Composite Pavements, User's Guide.* ERES Consultants, Champaign, IL.

Littleton, P. (2003) *Effect of Stress State on Concrete Slab Fatigue Resistance,* Masters thesis, University of Illinois, Urbana, IL.

Murdock, J.W. and Kesler, C.E. (1958), " Effect of Range of Stress on Fatigue Strength of Plain Concrete Beams," *Journal of the American Concrete Institute*, Vol. 30, No.2, pp.221-231.

Packard, R. G. (1973) *Design of Concrete Airport Pavement*. Engineering Bulletin EB050.03P. Portland Cement Association, Skokie, IL.

Packard, R. G. (1974) "Fatigue Concepts for Concrete Airport Pavement Design." *Journal of Transportation Engineering*, ASCE Vol. 100, No. TE3. American Society of Civil Engineers, New York, NY.

Parker, F., Barker, W.R., Gunkel, R.C., and Odom, E.C. (1979), *Development of a Structural Design Procedure for Rigid Airport Pavements,* Contract No. DOT FA73WAI-377, U.S. Army Engineer WES, Vicksburg, MS, 300 pp.

Raithby, K.D. and Galloway, J.W. (1974), "Effects of Moisture Condition, Age and Rate of Loading on Fatigue of Plain Concrete," *Abeles Symposium, Fatigue of Concrete*, ACI Publication SP-41, pp.15-34.

Rao, C.B., and Barenberg, E.J. (2000), "Fatigue Implication in Rigid Airport Pavements," *Proceedings of the 26th International Air Transportation Conference*, ASCE, San Francisco, CA, pp.298-312.

Roesler, J.R. (1998), *Fatigue of Concrete Beams and Slabs*, Ph.D. Thesis, University of Illinois, Urbana, Illinois.

Rollings, R. (1981), "Corps of Engineers Design Procedure for Rigid Airfield Pavements," *Proceedings of the Second International Conference on Concrete Pavement Design*, Purdue University, West Lafayette, IN, pp.185-198.

Rollings, R.S. (1986), *Field Performance of Fiber Reinforced Concrete Airfield Pavements,* DOT/FAA/PM-86/26, Federal Aviation Administration, Washington, D.C.

Rollings, R.S. (1988), *Design of Overlays for Rigid Airfield Pavements: Final Report,* DOT/FAA/PM-87/19, Federal Aviation Administration, Washington, D.C.

Rollings, R.S. and Witczak, M. (1990), "Structural Deterioration Model for Rigid Airfield Pavements," ASCE*, Journal of Transportation Engineering*, Vol. 116, No. 4, pp. 479-491.

Rollings, R.S. (2001), "Concrete Pavement Design: Its More Than a Thickness Design Chart," *Proceedings of the Seventh International Conference on Concrete Pavement Design*, Lake Buena Vista, FL, pp.281-296.

Rollings, R.S. (1998), "Evolution of the U.S. Military's Concrete Airfield Pavement Design Procedures," *Proceedings, Fourth International Workshop on Design Theories and Their Verification of Concrete Slabs for Pavements and Railroads*, Bucaco, Portugal, pp. 263-276.

Smith, K. and Roesler, J.R. (2003), "Review of Fatigue Models for Concrete Airfield Pavement Design," *ASCE Airfield Pavement Specialty Conference,* Las Vegas, NV, September 21-24, 26 pp.

Tepfers, R. and Kutti, T. (1979a), "Fatigue Strength of Plain, Ordinary, and Lightweight Concrete," *Journal of the American Concrete Institute*, Vol. 76, pp. 635-52.

Tepfers, R. (1979b), "Tensile Fatigue Strength of Plain Concrete," *Journal of the American Concrete Institute*, vol. 76, pp. 919-33.

Tepfers, R. (1982), "Fatigue of Plain Concrete Subjected to Stress Reversals," *ACI Publication SP-75*, pp. 195-217.

Westergaard, H.M. (1926), "Stresses in Concrete Pavements Computed by Theoretical Analysis," *Public Roads*, Vol. 7, No. 2, pp. 25-35.

Zollinger, D.G. and Barenberg, E.J. (1989), *Proposed Mechanistic Based Design Procedure for Jointed Concrete Pavements*, IHR-518, Illinois Cooperative Research Program, University of Illinois, Urbana, IL, 77 pp.